Accepted Manuscript

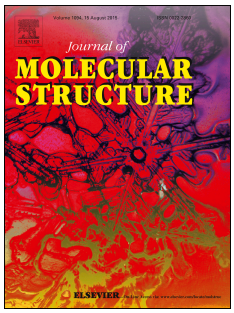

Synthesis, crystal structure, Hirshfeld surfaces analysis and anti-ischemic activity of cinnamide derivatives

Jian-gang Zhong, Jia-pei Han, Xiao-feng Li, Yi Xu, Yan Zhong, Bin Wu

PII: S0022-2860(17)31321-2

DOI: 10.1016/j.molstruc.2017.09.110

Reference: MOLSTR 24359

To appear in: *Journal of Molecular Structure*

Received Date: 27 June 2017

Revised Date: 27 September 2017

Accepted Date: 27 September 2017

Please cite this article as: J.-g. Zhong, J.-p. Han, X.-f. Li, Y. Xu, Y. Zhong, B. Wu, Synthesis, crystal structure, Hirshfeld surfaces analysis and anti-ischemic activity of cinnamide derivatives, *Journal of Molecular Structure* (2017), doi: 10.1016/j.molstruc.2017.09.110.

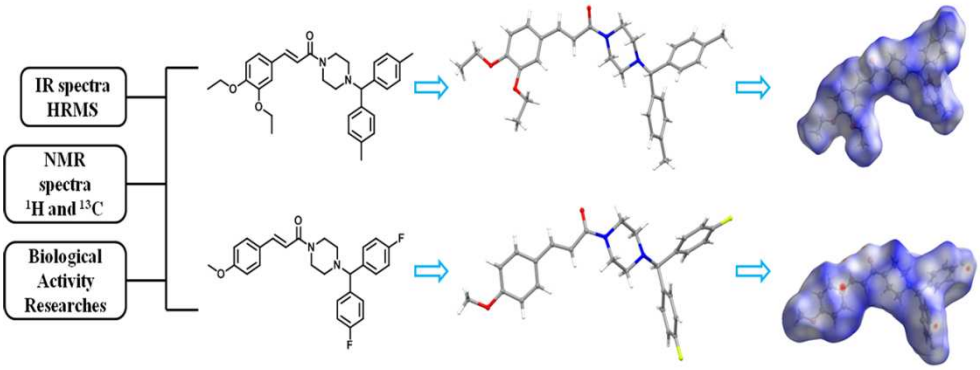

Graphical abstract

Synthesis, crystal structure, Hirshfeld surfaces analysis and anti-ischemic activity of cinnamide derivatives

Jian-gang Zhong[1], Jia-pei Han[1], Xiao-feng Li[2], Yi Xu[2], Yan Zhong[1,*], Bin Wu[2,*]

[1]School of Chemistry and Chemical Engineering, Southeast University, Nanjing 211189, China

[2]School of Pharmacy, Nanjing Medical University, Nanjing 211166, China

* Corresponding author. Tel/fax: +86 025 5209 0619.

E-mail: 101009944@seu.edu.cn (Y. Zhong); wubin@njmu.edu.cn (B. Wu).

Abstract

Two cinnamide derivatives, namely, (*E*)-1-(4-(bis(4-methylphenyl)-methyl)piperazin-1-yl)-3-(3,4-diethoxyphenyl)prop-2-en-1-one (**5**) and (*E*)-1-(4-(bis-(4-fluorophenyl)methyl)piperazin-1-yl)-3-(4-methoxyphenyl)prop-2-en-1-one (**6**), have been synthesized and characterized by IR spectra, High resolution mass spectra, ^{1}H NMR spectra, ^{13}C NMR spectra. The compound **5** is a novel compound and has never been reported in the literature. Their crystal structures were studied by single-crystal X-ray diffraction. They all crystallize in the monoclinic system. The single-crystal X-ray revealed that compound **5** has infinite X-shaped 1-D polymeric chains structure and compound **6** has a layered 3-D structure by intermolecular interactions. Hirshfeld surface analysis demonstrated the presence of H···H, O···H, C···H, F···H, C−H···π and π···π intermolecular interactions. In addition, the MTT assay results indicated that the compounds **5** and **6** display effective activities against neurotoxicity which is induced by glutamine in PC12 cells. The in vivo experiment

indicated that the compound **6** has a good protective effect on cerebral infarction.

Keywords: Cinnamide derivative; Crystal structure; Hirshfeld surface; MTT assay; Anti-ischemic activity

1. Introduction

Stroke, commonly known as cerebrovascular accident, is caused by cerebrovascular obstruction or rupture which will lead to brain blood circulation disorders and brain tissue function and structure damages. Stroke is the second primary reason of mortality and becomes the most common reason of long-term disability in the world [1-5]. There are two main types of stroke: ischemic, because of being short of blood flowing into the cerebrum, and hemorrhagic, because of bleeding into the cerebrum or into the ventricular system [6]. Especially, in China, ischemic stroke accounts for about 70% of total strokes [7-9]. Ischemic stroke mainly includes thrombotic cerebral infarction (cerebral thrombosis), embolic cerebral infarction, lacunar infarction, multiple cerebral infarction and transient ischemic attack [10,11]. The pathogenesis of ischemic stroke involves complex time and spatial cascade reactions that can initiate many links in the disease. Although the pathogenesis is not clear, scientists generally believe that activation of glutamate receptors which leads to increasing intracellular calcium concentration is the main cause of death in the infarct cells [8,12].

So far, the current methods of treating ischemic stroke are six major categories: antiplatelet therapy, thrombolytic therapy, anticoagulant therapy, neuroprotective therapy, traditional Chinese medicine treatment and other drug therapy. Among them,

traditional Chinese medicine treatment and other drug treatment are not obvious. Thrombolytic therapy can make the blood vessels recanalization, but it also produces reperfusion injury [13]. Hundreds of neuroprotective agents have been developed for stroke. Almost all of the neuroprotective agents are effective in animal experiments, however, the clinical effect is poor even ineffective or the serious side effects limit its clinical application. Therefore, the search for new neuroprotective agents has become the focus of current research.

Natural products are biologically interesting molecules that play an important role in modern drug discovery [14]. S.R. Kim et al. obtained some natural products by extracting dried roots of Scrophularia buergeriana [15]. Studies have shown that these compounds exhibit strong neuroprotective activity. Then the structure-activity relationship of these compounds indicated that the (*E*)-*p*-methoxycinnamoyl structure has neuroprotective activity [16]. Some literature reported that substituted benzhydrylpiperazine structures also have antioxidant neuroprotective activity [17].

Based on the above information, we used the splicing principle to incorporate cinnamoyl moiety and benzhydrylpiperazine structure into the same molecule, and found that cinnamide scaffold often affords neuroprotective compounds. Especially (*E*)-1-(4-(bis(4-fluorophenyl)methyl)piperazin-1-yl)-3-(4-methoxyphenyl)prop-2-en-1-one (compound **6** in this paper), which has the (*E*)-*p*-methoxycinnamoyl moiety, exhibited good neuroprotection in vitro [18]. In subsequent work, we selected **6** as lead compound, and designed and synthesized several novel series of cinnamide derivatives substituted with different functional groups to study of the substituent

variability influence on the biological activity. Compound **6** showed good neuroprotective activity at three test concentrations (0.1, 1.0, 10 μM) (protection > 40%) and exhibited better neuroprotection than positive control Edaravone.

In this study, compound **5** and **6** were synthesized and characterized by using different spectroscopic methods. The in vitro bioassay activity of compounds **5** and **6** was studied by MTT assay. Moreover, compound **6** was conducted on an animal experiment for further research.

2. Experimental section

2.1. General procedures

All chemicals were of analytical grade and used without further purification. Melting point was determined on a WRR-401 apparatus and was uncorrected. The ^{1}H and ^{13}C NMR spectra were recorded on a Bruker AV-500 instrument ($CDCl_3$ solution; TMS internal standard). High resolution mass spectra (HRMS) were obtained on a MALDI Micro MX instrument. IR was obtained on Bruker Tensor 27 FT-IR with KBr pellets. Fetal bovine serum (FBS) was got from HyClone (Logan, Utah, USA). 3-(4,5-Dimethylthiazol-2-yl)-2,5-diphenyltetrazolium bromide (MTT) was got from Sigma Chemical Company (Saint Louis, Missouri, USA).

2.2. Synthesis

*2.2.1. Synthesis of (E)-1-(4-(bis(4-methylphenyl)methyl)piperazin-1-yl)-3-(3,4-diethoxyphenyl)prop-2-en-1-one **5***

The synthesis step of the target compound is shown in Scheme 1. The substituted 1-benzhydrylpiperazine **2** was prepared from substituted benzophenone **1** according to

the reference [19]. The substituted cinnamic acid **4** was synthesized from substituted benzaldehydes **3** by the Knoevenagel reactions [20]. The detailed synthesis step of the target compound is shown below.

A stirred solution of compound (**4**, 5 mmol) in dichloromethane (15 mL) was treated dropwise with oxalyl dichloride (2.5 mL) and N,N-dimethylformamide (2 drop), continuing to stir at room temperature for 1 hour. After completion of the reaction, the solvent was evaporated under reduced pressure. The compound (**2**, 6 mmol) and triethylamine (3 mL) were placed in tetrahydrofuran (30mL) and the residue that was dissolved in tetrahydrofuran (15 mL) of the previous step was added dropwise at 0 □. Then the reaction solution was stirred overnight at ambient temperature. The solution was removed under reduced pressure for a small volume after completion of the reaction and the residue was purified by column chromatography (66% EtOAc in petroleum ether) to yield the white solid compound **5** (1.58 g, 63.2%). m.p.: 131~133 □. ^{1}H NMR ($CDCl_3$) δ: 1.42~1.48 (m, 6H, 2**CH$_3$**CH$_2$O), 2.26~2.29 (s, 6H, 2CH$_3$-Ph), 2.40~2.43 (m, 4H, N(CH$_2$)$_2$), 3.65~3.72 (m, 4H, CON(CH$_2$)$_2$), 4.05~4.13 (m, 4H, 2CH$_3$**CH$_2$**O), 4.19 (s, 1H, CH(Ph)$_2$), 6.64 (d, *J* = 15.3 Hz, 1H, COCH=), 6.81~7.30 (m, 11H, Ar-H), 7.55 (d, *J* = 15.3 Hz, 1H, PhCH=). ^{13}C NMR ($CDCl_3$) δ: 14.72, 21.16, 42.96, 45.99, 64.67, 75.25, 112.36, 112.95, 114.70, 121.69, 127.63, 128.24, 129.16, 136.54, 139.31, 142.49, 148.69, 150.31, 165.47. IR (KBr, cm^{-1}): 3060.2, 3018.7, 2980.7, 2814.2, 1637.9, 1588.5, 1512.7, 1458.7, 1429.5, 1266.5, 1234.0, 1138.4, 1043.2, 799.0. HRMS (ESI, m/z): Calcd. for $C_{32}H_{38}N_2O_3Na$ [M + Na$^+$] 521.2780. Found: 521.2768.

*2.2.2. Synthesis of (E)-1-(4-(bis(4-fluorophenyl)methyl)piperazin-1-yl)-3-(4-methoxyphenyl)prop-2-en-1-one **6***

In similar procedure, the target compound **6** was obtained in a 56% yield as a white solid. m.p.: 170～172 ℃. ^{1}H NMR ($CDCl_3$) δ: 2.38~2.41 (m, 4H, $N(CH_2)_2$), 3.68 (br, 4H, $CON(CH_2)_2$), 3.82 (s, 3H, OCH_3), 4.25 (s, 1H, $CH(Ph)_2$), 6.67 (d, *J* = 15.3 Hz, 1H, COCH=), 6.86~7.45 (m, 12H, Ar-H), 7.60 (d, *J* = 15.3 Hz, 1H, PhCH=). ^{13}C NMR ($CDCl_3$) δ: 42.20, 45.81, 45.90，51.53，51.59，51.90，51.94，55.25, 74.19, 114.15, 114.42, 115.34，115.62，127.94, 129.13, 129.19，129.23, 137.59, 142.38, 160.23, 160.79，163.49, 165.56. IR (KBr, cm^{-1}): 3075.5, 3028.0, 2969.7, 2821.3, 1647.4, 1600.8, 1573.1, 1510.4, 1449.5, 1279.6, 1221.2, 1173.8 1003.4, 823.7. HRMS (ESI, m/z): Calcd. for $C_{27}H_{26}F_2N_2O_2Na$ [M + Na^+] 471.1860. Found: 471.1816.

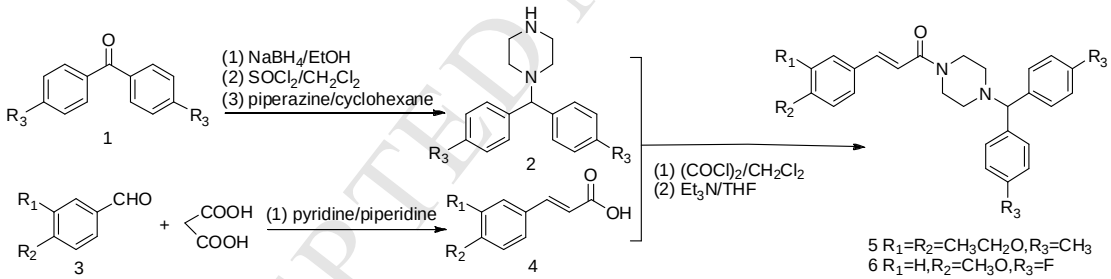

Scheme 1. Synthesis of the title cinnamide compounds **5** and **6**.

2.3. Crystal structure determination

Suitable crystals were obtained by slow evaporation in ethanol (compound **5**) or a mixture of chloroform and cyclohexane (compound **6**) solution at room temperature. The single-crystal X-ray diffraction data of title compounds **5** and **6** were collected at 293(2)K with graphite-monochromated Mo Kα radiation (λ = 0.71073 Å) on an Enraf-Nonius CAD4/PC four-circle diffractometer, using the ω-scan mode [21]. The structure was decided by using SHELXS-97 and refined against F^2 by full-matrix

least-squares method [22]. Hydrogen atoms were generated geometrically. The Diamond [23] and Mercury programs [24] were used to describe the molecular structures. The crystal data and parameters of the crystal structure refinement statistics were summarized in Table 1.

Table 1 The crystal data and structure refinement for compounds **5** and **6**.

Compound	**5**	**6**
Formula	$C_{32}H_{38}N_2O_3$	$C_{27}H_{26}F_2N_2O_2$
Formula weight	498.64	448.50
Crystal system	Monoclinic	Monoclinic
Space group	$P2_1/c$	$P2_1/n$
a/Å	13.592(3)	10.171(2)
b/Å	21.263(4)	16.280(3)
c/Å	9.939(2)	14.053(3)
β/°	90.63(3)	97.12(3)
V/Å^3	2872.3(10)	2309.0(8)
Z	4	4
D_{calc} (mg m^{-3})	1.153	1.290
T/K	293(2)	293(2)
μ (mm^{-1})	0.074	0.092
Cryst dimensions	0.3×0.2×0.1	0.3×0.2×0.2
No. of reflections collected	5268	4247
No. of unique reflections	2485	2946
No. of parameters	335	298
Goodness-of-fit (GOF) on F^2	1.003	1.006
R_1,wR_2 ($I > 2\sigma(I)$)	0.0683, 0.1569	0.0542, 0.1460
R_1, wR_2 (all data)	0.1610, 0.1996	0.0827, 0.1661
CCDC NO.	867525	806575

2.4. Pharmacology

2.4.1. In vitro experiment

In order to investigate the in vitro anti-ischemic activity, the title compounds **5** and **6** were screened in Glu-induced PC12 cells. The cellular viability was assessed by MTT assay [25-28].

PC12 cells were vaccinated in 96-well plates (104 cells/pore). Dulbecco's

modified Eagle's Medium (DMEM) containing 10% FBS was put into the cell incubator under the condition of 5% CO_2. When the degree of cell fusion reached about 60% under the microscope after 24 hours of cultivating, the culture medium was removed. Glutamine at a concentration of 10 mmol/mL was incubated in serum-free DMEM at 37 ℃ for 1 hour. Then glutamine (10 mmol/L) with compounds **5** and **6** (0.1, 1, 10 μmol/L) or Edaravone (90 μmol/L) were cultivated in serum-free DMEM for 24 hours separately. The culture medium was removed. The MTT (100 μL, 0.5 mg/mL) was added to each culture well at 37 ℃. Finally, 100 μL of DMSO solution was added to each well after 4 hours. The cells were dissolved in Scroll instrument to read with a microplate reader (the measurement wavelength was 570 nm and the reference wavelength was 630 nm) [29, 30]. Each sample is made of five holes.

2.4.2. In vivo experiment

The *in vivo* anti-ischemic activity of the title compound **6** was tested using middle cerebral artery occlusion (MCAO) model. Infarction area was assessed by TTC staining assay [31, 32].

Kunming mice of both sexes were randomly divided into 6 groups (10 mice per group) which are sham-operated group, MCAO model group, C6/4 group (4 mg/Kg), C6/12 group (12 mg/Kg), C6/36 group (36 mg/Kg) and Edaravone group (6 mg/Kg) respectively. Focal cerebral ischemia was induced according to the MCAO method. Reperfusion was directed by using suture 2 hours after MCAO. After 24 h of reperfusion, the brain of the rats was isolated to estimate the infarct size.

Sham-operated groups were performed in the same situation to avoid the influence of the suture. The brain tissues were stained by TTC, which were photographed immediately with an HD digital camera, and infarction area was analyzed with Image-pro Plus Version 5.1.

3. Result and discussion

3.1. Chemistry

Substituted benzaldehydes **1** were used as starting materials, which were treated with malonic acid to afford substituted cinnamic acid **4**. Cinnamic acid chlorides, which were obtained by oxalyl dichloride in dichloromethane at room temperature, were allowed to react with **2** in the presence of triethylamine to afford the target compounds **5** and **6**. The chemical structures of these compounds were confirmed by spectroscopic methods.

*3.2. Crystal structures of compounds **5** and **6***

The single-crystal X-ray diffraction study reveals that compound **5** crystallizes as colorless block crystals in the monoclinic system in space group $P2_1/c$ with Z = 4, the asym-metric unit (ASU) consisting of an entire compound **5** molecular (Fig. 1a). The title molecule exists in an *E* configuration with respect to the C21=C22 ethene bond (distance of 1.317(4) Å). The piperazine ring adopts a chair conformation. The geometrical parameters for the hydrogen bonds in the two moleculars are summarized in Table 2.

The crystal can be described as every two molecules of compound **5** are crossed together to form a “X” structure (Fig. 1b). The X structures are further stacked by

C−H···O intermolecular interactions, with average distances of 3.358 Å between the carbonyl oxygen of one molecule and the carbon (C17, C21 and C14) of another in the adjacent X units, into an interlaced chain structure (Fig. 1c). The plane separation between the stacked compound **5** molecules in the adjacent X units is 9.939 Å. Additionally, these molecules are connected in an $\cdots X_1X_{-1}X_1X_{-1}\cdots$ fashion by means of C−H···O (distance of 3.486 Å for the carbonyl group and 3.531 Å for the ethoxy group) and C−H···π (distance of 3.571 Å) interactions to form infinite X-shaped 1-D polymeric chains (Fig. 1d). The two X units in the chains form a head-to-tail type interaction and every two molecules in the "X" units parallel with each other are reverse.

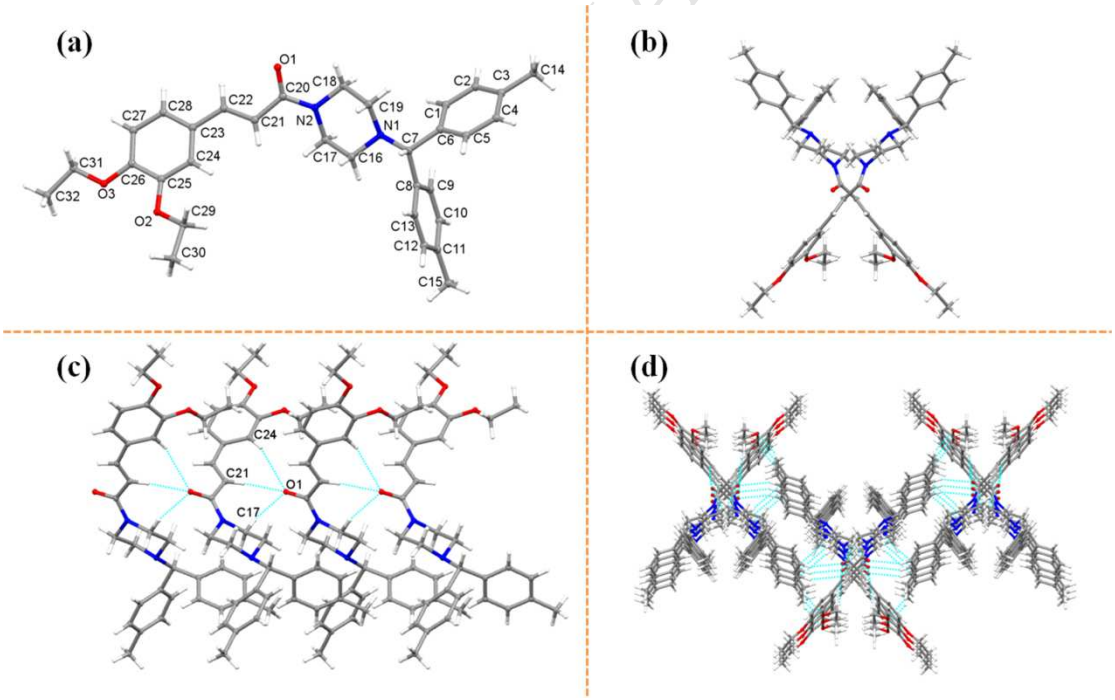

Fig. 1 (a) Molecular structure of **5** with atom labeling of the asymmetric unit; (b) two compound **5** molecules are crossed together to form a "X" structure; (c) The X structures are further stacked by C−H···O intermolecular interactions; (d) infinite X-shaped 1-D polymeric chains.

The single-crystal X-ray diffraction study reveals that compound **6** crystallizes as colorless block crystals in the monoclinic system in space group $P2_1/n$ with Z = 4, the

asym-metric unit (ASU) consisting of an entire compound **6** molecular (Fig. 2a). The title molecule also has an *E* configuration and a chair conformation.

The structure can be described as follows: the molecules of compound **6** are connected by means of C14−H14A···F2 (distance of 3.207 Å) interactions to form infinite 1-D chains structure (Fig. 2b). As shown in Fig. 2c, The 1-D chain structure formed a 2-D structure through two hydrogen bonds C8-H8···O2 (distance of 3.453 Å) where the phenyl ring acts as an H donor and the corresponding carbonyl group of the adjacent molecule acts as an H acceptor. The 2-D structure are further stacked in a parallel fashion to form a layered 3-D structure by C18−H18···F2 (distance of 3.472 Å) and π···π (distance of 3.672 Å) interactions (Fig. 2d).

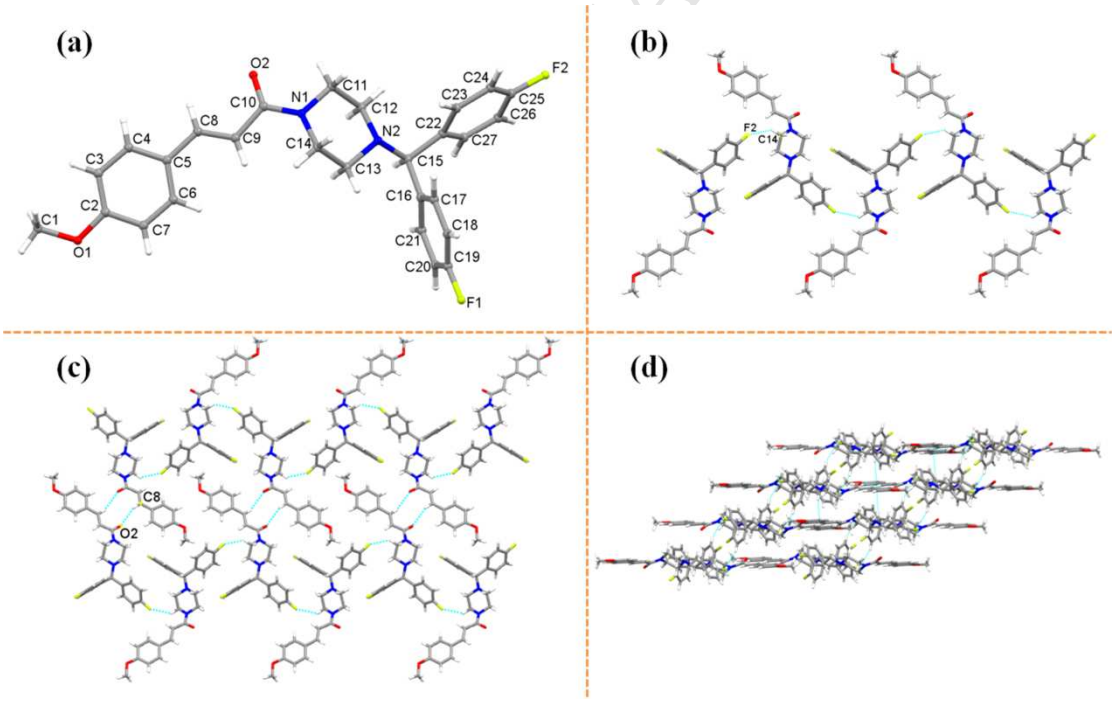

Fig. 2 (a) Molecular structure of **6** with atom labeling of the asymmetric unit; (b) 1-D chain structure of compound **6**; (c) perspective view of 2-D structure of compound **6**; (d) 3-D pack structure of compound **6**.

Table 2 Geometrical parameters for the hydrogen bonds in the compounds **5** and **6**.

D−H···A	D−H(Å)	D···A(Å)	H···A(Å)	∠D−H···A(°)
compound **5**				
C4–H4···O1	0.930	3.486	2.696	143.28

C17–H17B···O1	0.969	3.288	2.365	158.90
C21–H21···O1	0.930	3.281	2.357	171.95
C24–H24···O1	0.930	3.506	2.698	145.81
C14–H14B···O2	0.961	3.531	2.647	153.07
compound **6**				
C8–H8···O2	0.930	3.453	2.587	155.12
C14–H14A···F2	0.969	3.207	2.452	134.59
C18–H18···F2	0.930	3.472	2.597	156.95

3.3. Hirshfeld surfaces analysis

The intermolecular interactions of compounds **5** and **6** can be visualized by Hirshfeld surface analysis which is often used to explore molecular crystals [33-35]. As is shown in Fig. 3, the Hirshfeld surfaces of the two moleculars have been mapped over d_{norm}(-0.304 to 1.552, -0.131 to 1.416 Å for moleculars **5** and **6**, separately) and the fingerprint plots of moleculars **5** and **6** are illustrated in Fig. 4. For the compounds **5** and **6**, the red regions mainly indicate strong O···H and F···H interactions and the green color regions in the 2-D fingerprint plots mainly represent H···H, O···H, and F···H interactions.

The O···H intermolecular interactions look like a “bat”, which contribute 10.1% and 10.2% to the total Hirshfeld surfaces for compounds **5** and **6.** The F···H interactions comprise 16.2% of the total Hirshfeld surfaces, which is the red area on the d_{norm} surface for compound **6**. The H···H interactions have a more significant contribution to the total Hirshfeld surfaces of compounds **5** and **6**, comprising 67.8% and 44.9% and reflect in the middle of the 2-D fingerprint plots. The “butterfly” are identified as a consequence of C···H interactions, contributing 21.4%, 24.6% to the total Hirshfeld surfaces for compounds **5** and **6** at the upper right corner of the fingerprint plots**.** The C···C interactions is belong to π···π interactions and have a

lower contribution to the two moleculars, of 0.2%, and 2.2% in the total Hirshfeld surfaces, respectively. The percentage of C···O contacts of **5** and **6** is 0.2%, and 0.1%, respectively. Besides the contacts mentioned above, the presence of F···C, F···F, N···H and other interactions is summarized in Table 3.

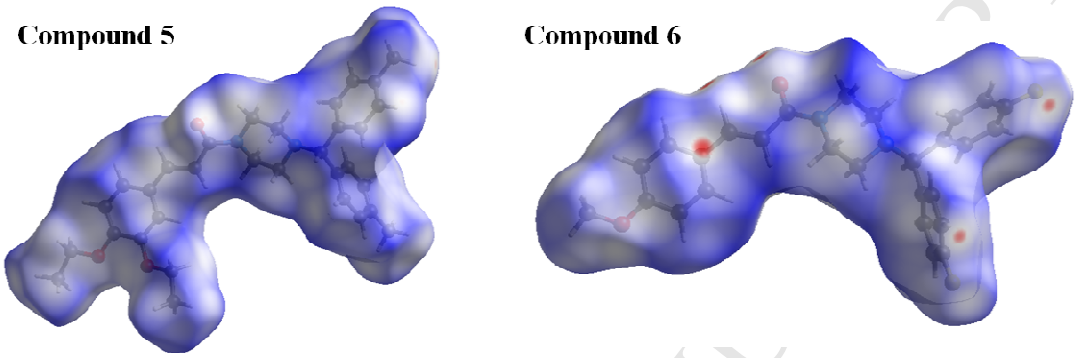

Fig. 3 Hirshfeld surface mapped with d_{norm} for the compounds **5** and **6**.

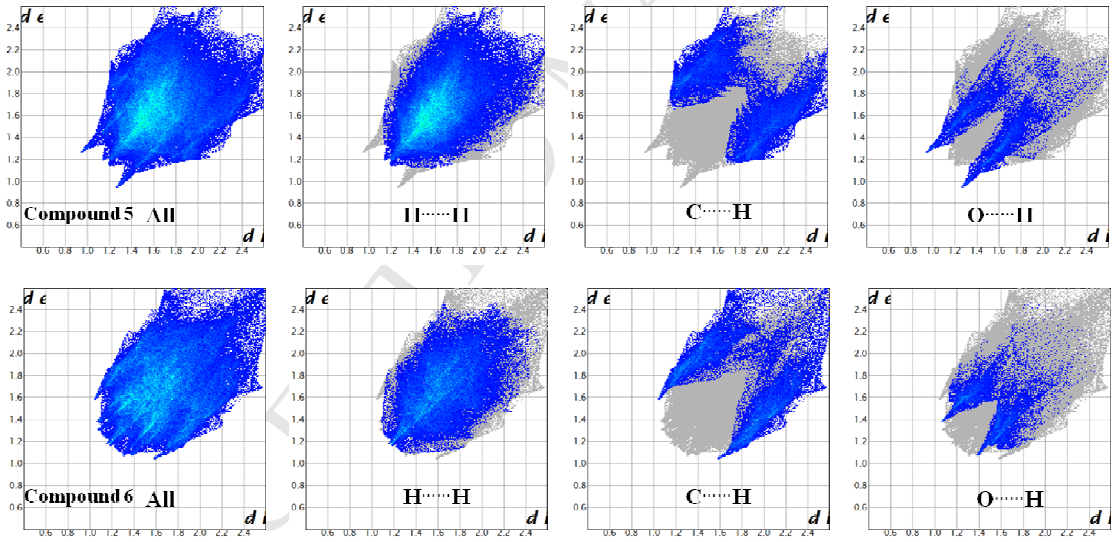

Fig. 4 The 2D fingerprint plots of the compounds **5** and **6.**

Table 3 The percentages of the various interactions contributions to the total Hirshfeld surface area of the compounds **5** and **6**.

Interactions	Percentage (%)	
	Compound **5**	Compound **6**
H···H	67.8	44.9
O···H	10.1	10.2
C···H	21.4	24.6
N···H	0.2	0.4
C···C	0.2	2.2

C···O	0.2	0.1
F···C	—	0.7
F···H	—	16.2
F···F	—	0.1
other	0.1	0.6

3.4. Pharmacological evaluation

3.4.1. MTT assay

The inhibitory effect of the compounds **5** and **6** on glutamate-induced PC12 cell injury was performed by MTT assay. As shown in Fig. 5, we can clearly find the compound 5 has a weak inhibitory effect on glutamate-induced PC12 cells injury in a dose-dependent manner. Although the dose-effect relationship of the compound **6** is not obvious, it could significantly inhibit the damage of PC12 cells induced by glutamate, is stronger than the positive control drug Edaravone. No matter in the previous work or the new work, the inhibitory effect of the compounds on glutamate-induced PC12 cell injury was performed by MTT assay and compared to Edaravone. Cell protection of compound **6** at four test concentrations (0.1, 1.0, 10, 100 μM) was 91.2%, 70.4%, 97.4% and 4.8%, respectively (Chinese Chemical Letters 2008) [18]. Cell protection of compound **6** at three test concentrations (0.1, 1.0, 10 μM) was 71.01%, 49.66%, and 77.75%, respectively. No matter in the previous work or now, this compound showed good neuroprotective activity at three test concentrations (0.1, 1.0, 10 μM) (protection > 40%) and exhibited better neuroprotection than Edaravone. Next, we conducted an animal experiment on compound **6** for further research.

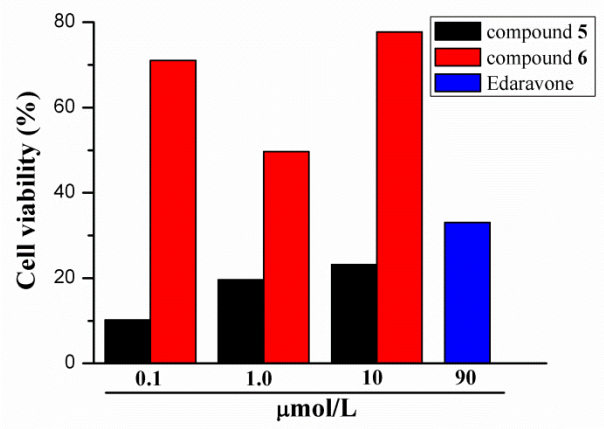

Fig. 5 The inhibitory effect of the compounds **5** and **6** on glutamate-induced PC12 cell injury, the cell viability (%) of the compounds **5** and **6** in three dose groups is 10.18% (0.1 μmol/L,**5**), 19.62% (1.0 μmol/L,**5**), 23.17% (10 μmol/L,**5**), 71.01% (0.1 μmol/L,**6**), 49.66% (1.0 μmol/L,**6**) and 77.75% (10 μmol/L,**6**) respectively; the cell viability (%) of the Edaravone is 33.04% (90 μmol/L).

3.4.2. Anti-ischemic activity

The model of cerebral ischemia-reperfusion was established by middle cerebral artery occlusion (MCAO), and the pharmacological evaluation of compound **6** was performed. After the experiment, the color of the brain tissue infarction area became white without staining, but the normal brain tissue was stained with dark-red (Fig. 6a). As shown in Fig. 6b, the area of cerebral infarction in each dose group was significantly lower than that in MCAO model group ($p < 0.01$). When compound **6** was administered at a dose of 36 mg/kg, the infarction area reached to the maximal reduction with an infarction area of 11.12±3.3%. This indicated that compound **6** has a good protective effect on MCAO cerebral infarction.

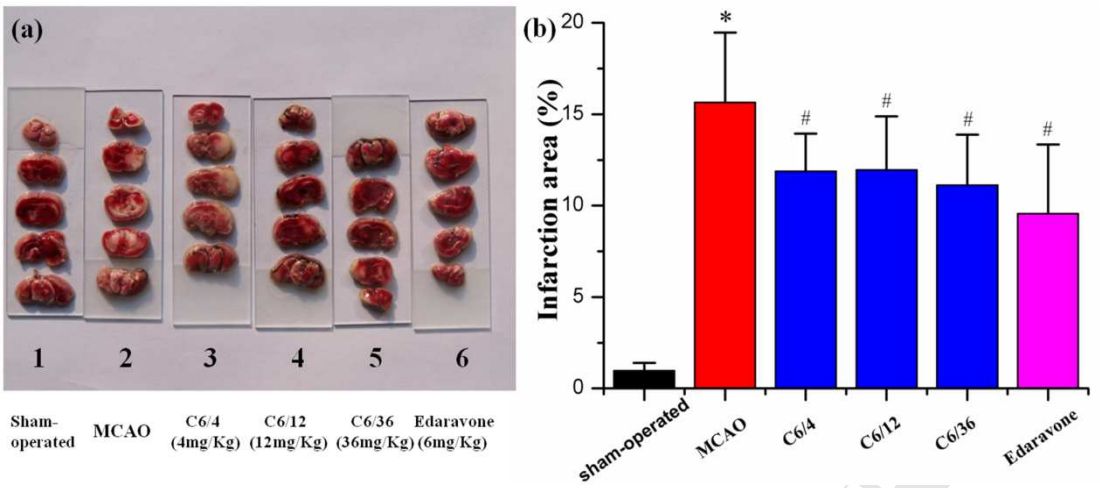

Fig. 6 (a) The infarction area on each section of rat brain was determined on digital images using a computerized image analyzer, and infarction area was assessed calculated; (b) the infarction area (%, $\bar{X}$ ± SD) is as follows: 0.97 ± 0.42% (sham-operated), 15.64 ± 3.83%* (MACO), 11.87 ± 2.07%$^{\#}$ (C6/4), 11.96 ± 2.92%$^{\#}$ (C6/12), 11.12 ± 2.76%$^{\#}$ (C6/36) and 9.56 ± 3.78%$^{\#}$ (Edaravone). *$P < 0.01$, compared with sham-operated; $^{\#}P < 0.01$, compared with MACO.

4. Conclusion

In this work, we have designed and synthesized two cinnamide derivatives. The compound **5** is a novel compound, while the compound **6** has been reported in our previous study. These compounds were characterized by IR spectra, High resolution mass spectra, ^{1}H NMR spectra, ^{13}C NMR spectra and single-crystal X-ray diffraction. Crystal structures analysis revealed that the stacking motif of the compound **5** is constructed by C−H···O and C−H···π interactions and that of the compound **6** is constructed by C−H···O, C−H···F and π···π stacking interactions. Hirshfeld surface analysis demonstrated the presence of H···H, O···H, C···H, F···H, C−H···π and π···π intermolecular interactions. Furthermore, the MTT assay results indicated that the compound **5** has a weak inhibitory effect on glutamate-induced PC12 cells injury in a dose-dependent manner, while the compound **6** significantly inhibits the damage of PC12 cells. Moreover, the compound **6** was conducted on an animal experiment for

further research. The results revealed that compound **6** has a good protective effect on MCAO cerebral infarction. Finally, the further research will be in the following paper on the basis of the present study.

Acknowledgements

This work was supported by the National Natural Science Foundation of China (No. 81371451) and the Natural Science Foundation of Jiangsu Province (No. BK20131390).

Supporting information

CCDC 867525 and 806575 contains the supplementary crystallographic data for **5** and **6**. These data can be obtained free of charge via http://www.ccdc.cam.ac.uk/ conts/retrieving.html, or from the Cambridge Crystallographic Data Centre, 12 Union Road, Cambridge CB2 1EZ, UK; fax: (+44) 1223-336-033; or e-mail: deposit@ccdc.cam.ac.uk.

References

[1] R.W.V. Flynn, R.S.M. MacWalter, A.S.F. Doney, The cost of cerebral ischaemia, Neuropharmacology. 55 (2008) 250-256.

[2] Y. Gu, K. Zhao, X. Luan, Z. Liu, Y. Cai, Q. Wang, B. Zhu, J. He, Association between Serum Magesium Levels and Depression in Stroke Patients, Aging. Dis. 7 (2016) 687-690.

[3] M. Liu, B. Wu, W. Wang, L. Lee, S. Zhang, L. Kong, Stroke in China: epidemiology, prevention, and management strategies, Lancet Neurol. 6 (2007) 456-64.

[4] V.L. Feigin, Stroke epidemiology in the developing world, Lancet. 365 (2005) 2160-2161.

[5] K.K. Snarska, H. Bachórzewska-Gajewska, K. Kapica-Topczewska, W. Drozdowski, M. Chorąży, A. Kułakowska, J. Małyszko, Hyperglycemia and diabetes have different impacts on outcome of ischemic and hemorrhagic stroke, Arch. Med. Sci. 13 (2017) 100-108.

[6] S.H. Koh, H.H. Park, Neurogenesis in Stroke Recovery, Transl. Stroke. Res. 8 (2017) 3.

[7] Y. Zhong, Z. Xu, Y. Wang, Y. Xu, P. Li, B. Wu, Synthesis, Crystal Structure and Anti-ischaemic Activity of (E)-1-{4-[Bis(4-methoxy-phenyl)methyl]piperazin-1-yl}-3-(4-chlorophenyl)-prop-2- en-1-one, S. Afr. J. Chem. 67(2014) 214-217.

[8] Y. Zhong, Z. Xu, Y. Wang, Y. Xu, P. Li, B. Wu, Synthesis and biological evaluation of aryloxyacetamide derivatives as neuroprotective agents, Bioorg. Med. Chem. Lett. 26 (2016) 2526-2530.

[9] S. Zhang, Z. Liu, Y. Liu, Y. Wang, T. Liu, X. Cui, Prevalence of stroke and associated risk factors among middle-aged and older farmers in western China, Environ. Health. Prev. Med. 22 (2017) 6.

[10] W.R. Schabitz, M. Fisher, Perspectives on neuroprotective stroke therapy, Biochem. Soc. T. 34 (2006) 1271-1276.

[11] J. Wardas, Neuroprotective role of adenosine in the cns, Pol. J. Pharmacol. 54 (2002) 313.

[12] M. Steven, W. John, Glutamate and the pathophysiology of hypoxic-ischemic brain damage, Ann. Neurol. 19 (2010) 105-111.

[13] L. He, X. Chen, M. Zhou, D. Zhang, J. Yang, M. Yang, D. Zhou, Radix/rhizoma notoginseng extract (sanchitongtshu) for ischemic stroke: A randomized controlled study, Phytomedicine. 18 (2011) 437-42.

[14] C. Srinivas, C. Kumar, B. Raju, V. Rao, V. Naidu, S. Ramakrishna, P. Diwan, First stereoselective total synthesis and anticancer activity of new amide alkaloids of roots of pepper, Bioorg. Med. Chem. Lett. 19 (2009) 5915-5918.

[15] S.R. Kim, Y.C. Kim, Neuroprotective phenylpropanoid esters of rhamnose isolated from roots of Scrophularia buergeriana, Phytochemistry. 54 (2000) 503-509.

[16] S.R. Kim, K.Y. Lee, K.A. Koo, S.H. Sung, N.G. Lee, J. Kim, Y.C. Kim, Four New Neuroprotective Iridoid Glycosides from Scrophularia buergeriana Roots, J. Nat. Prod. 65 (2002) 1696-1699.

[17] N. Sugiyama, F. Akahoshi, S. Kuwahara, M. Kajii, Y. Sakaue, H. Yakumaru, M. Sugiura, C. Fukaya, Synthesis and Topical Antiinflammatory and Antiallergic Activities of Antioxidant o-Aminophenol Derivatives, J. Med. Chem. 37 (1994) 1977-1982.

[18] B. Wu, L. Zhou, H.H. Cai, Synthesis and neuroprotective properties of novel cinnamide derivatives, Chinese Chem. Lett. 19 (2008) 1163-1166.

[19] L. Wang, H. Jiang, Y. Zhou, B. Liu, Z. Ji, Synthesis and antiallergic activities of diphenylmethylpiperazine deravatives, Chin. J. Med. Chem. 12 (2002) 125-129.

[20] K. Tanaka, K. Matsuo, A. Nakanishi, T. Hatano, H. Izeki, Y. Ishida, W. Mori, Syntheses and anti-inflammatory and analgesic activities of Hydroxamic Acid and Acid Hydrazides, Chem. Pharm. Bull. 31 (1983) 2810-2819.

[21] O. Yarnton, Agilent Technologies (formerly Oxford Diffraction), England. 2012.

[22] G.M. Sheldrick, SHELXS97: Programs for Crystal Structure Analysis, University of Göttingen, Germany. 1997.

[23] K. Brandenburg, DIAMOND: Crystal and Molecular Structure Visualization, Version 3.1b, Crystal Impact GbR, Bonn, Germany. 2006.

[24] Mercury 2.3 Supplied with Cambridge Structural Database, CCDC, Cambridge, U.K. 2003–2004.

[25] Y. Zhong, Z. Xu, Y. Wang, Y. Xu, P. Li, B. Wu, Synthesis, Crystal Structure and Anti-ischaemic Activity of (E)-1-{4-[Bis(4-methoxy-phenyl)methyl]piperazin-1-yl}-3-(4-chlorophenyl)-prop-2- en-1-one. Chin. J. Struct. Chem. 34 (2015) 681-687.

[26] S.J. Park, K.W. Nam, H.J. Lee, E.Y. Cho, U. Koo, W. Mar, Neuroprotective effects of an alkaloid-free ethyl acetate extract from the root of Sophora flavescens Ait. Against focal cerebral ischemia in rats, Phytomedicine, 16 (2009) 1042-1051.

[27] S.W. Ma, H.X. Liu, H.Y. Jiao, L.Y. Wang, L.Y. Chen, J. Liang, M. Zhao, X.T. Zhang, Neuroprotective effect of ginkgolide K on glutamate-induced cytotoxicity in PC 12 cells via

inhibition of ROS generation and Ca^{2+} influx. Neurotoxicology, 33 (2012) 59-69.

[28] T. Mosmann, Rapid Colorimetric Assay for Cellular Growth and Survival: Application to Proliferation and Cytotoxicity Assays, J. Immunol. Methods. 65 (1983) 55-63.

[29] T. Terauchi, T. Doko, M. Yonaga, A. Kajiwara, T. Niidome, R. Taguchi, T. Kume, A. Akaike, H. Sugimoto, Synthesis and neuroprotective effects of serofendic acid analogues, Bioorg. Med. Chem. Lett. 16(2006) 5080-5083.

[30] A. Akaike, Y. Tamura, Y. Sato, T. Yokota, Protective effects of a vitamin B_{12} analog, methylcobalamin, against glutamate cytotoxicity in cultured cortical neurons, Eur. J. Pharmacol. 241 (1993) 1-6.

[31] Y. Zhang, X. Wang, Z. Xu, Z. Liu, Q. Ni, X. Chu, M. Qiu, A. Zhao, W. Jia, Protective effect of flavonoids from Scutellaria baicalensis Georgi on cerebral ischemia injury, J. Ethnopharmacol. 108 (2006) 355-360.

[32] Q. Zhang, X. Dong, J. Xia, K. Xu, Z. Xu, Obestatin Plays Beneficial Role in Cardiomyocyte Injury Induced by Ischemia-Reperfusion In Vivo and In Vitro, Med. Sci. Monitor. 23 (2017) 2127-2136.

[33] J.J. Mckinnon, A.S. Mitchell, M.A. Spackman, Hirshfeld Surfaces: A New Tool for Visualising and Exploring Molecular Crystals, Chem. Eur. J. 4 (1998) 2136-2141.

[34] M.A. Spackman, J.J. McKinnon, Fingerprinting intermolecular interactions in molecular crystals, CrystEngComm. 4 (2002) 378-392.

[35] J.J. Mckinnon, A.S. Mitchell, M.A. Spackman, Novel tools for visualizing and exploring intermolecular interactions in molecular crystals, Acta Crystallogr. B. 60 (2004) 627-68.

Highlights

- Two cinnamide derivatives have been synthesized and characterized.
- Their crystal structures were studied by single-crystal X-ray diffraction.
- Intermolecular interactions of compounds have been quantificationally visualized.
- The bioassay activity of the compounds in vitro and in vivo was studied.